Amakusamine from a *Psammocinia* sp. Sponge: Isolation, Synthesis, and SAR Study on the Inhibition of RANKL-Induced Formation of Multinuclear Osteoclasts

Yuka Maeyama,[†] Yuta Nakashima,[‡] Hikaru Kato,[†] Yuki Hitora,[†] Kazuhiko Maki,[†] Natsumi Inada,[†] Shunya Murakami,[†] Tomoaki Inazumi,[§] Yuji Ise,[⊥] Yukihiko Sugimoto,[§] Hayato Ishikawa,[#] and Sachiko Tsukamoto[†,*]

[†] *Department of Natural Medicines, Graduate School of Pharmaceutical Sciences, Kumamoto University, Kumamoto 862-0973, Japan*

[‡] *Graduate School of Science and Technology, Kumamoto University, Kumamoto 860-8555, Japan*

[§] *Department of Pharmaceutical Biochemistry, Graduate School of Pharmaceutical Sciences, Kumamoto University, Kumamoto 862-0973, Japan*

[⊥] *Sesoko Station, University of the Ryukyus, 3422 Sesoko, Motobu, Okinawa 905-0227, Japan*

[#] *Graduate School of Pharmaceutical Sciences, Chiba University, Chiba 260-8675, Japan*

*Corresponding Author

E-mail address: sachiko@kumamoto-u.ac.jp (S. Tsukamoto).

ABSTRACT: A simple methylenedioxy dibromoindole alkaloid, amakusamine (**1**), was isolated from a marine sponge of the genus *Psammocinia*, and its structure was determined from spectroscopic data, time-dependent density-functional theory (TDDFT) calculations, and synthesis. Compound **1** inhibited the receptor activator of nuclear factor-κB ligand (RANKL)-induced formation of multinuclear osteoclasts with an IC_{50} value of 10.5 μM in RAW264 cells. The structure–activity relationship (SAR) of **1** was also investigated with synthetic derivatives.

Marine organisms are known to be rich sources of biologically active compounds.[1] In particular, marine invertebrates such as sponges, tunicates, and bryozoans produce high levels of cytotoxic metabolites compared to terrestrial plants and microorganisms and have therefore been considered as potential sources of natural therapeutic agents.[2] Among the various structural classes, brominated compounds, which have been found in marine environments, exhibit bioactivities against diverse disease targets.[3] During our search for new compounds from marine sponges, LC-MS analysis indicated the presence of a new compound with two bromine atoms in an extract from a *Psammocinia* sp. sponge collected in Amakusa (Kumamoto, Japan). Then, we isolated the brominated compound and found that it inhibited the receptor activator of nuclear factor-κB ligand (RANKL)-induced formation of multinuclear osteoclasts in RAW264 cells. Homeostasis of bone is regulated by the balance of bone resorption by osteoclasts and bone formation by osteoblasts,[4-6] and its imbalance causes osteoporosis, rheumatoid arthritis, and periodontal disease.[7] Previous studies showed that a monocyte/macrophage lineage is differentiated to mononuclear osteoclasts by stimulus of RANKL and subsequently changed to giant multinuclear osteoclasts by cell fusion.[4-6] Therefore, the inhibitors of differentiation and cell fusion are drug candidates for prevention and treatment of osteoclast-related diseases. Here, we report the isolation, structure determination, synthesis, and biological activity of a new methylenedioxy dibrominated indole alkaloid, amakusamine (**1**). The structure–activity relationship (SAR) of **1** was also assessed with synthetic derivatives.

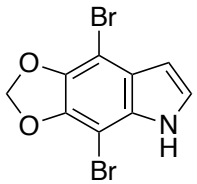

1

RESULTS AND DISCUSSION

The presence of two bromine atoms in **1** was indicated by ion peaks at *m/z* 316, 318, and 320 $[M - H]^-$ in a ratio of 1:2:1, and the molecular formula of $C_9H_5Br_2NO_2$ was determined by HRESIMS. The ^1H NMR spectrum of **1** in $CDCl_3$ showed four signals: an exchangeable NH proton [δ_H 8.30 (br s)], two mutually-coupled olefin protons [δ_H 7.15 (br s) and 6.55 (br s)], and a deshielded singlet proton [δ_H 6.07 (2H, s)] (Table 1). The ^{13}C NMR spectrum showed two protonated olefin carbons [δ_C 123.5 (C-2) and 103.9 (C-3)], a deshielded methylene carbon [δ_C 101.5 (C-10)], and six non-protonated olefin carbons [δ_C 142.7 (C-5), 141.4 (C-6), 129.4 (C-8), 122.9 (C-9), 91.6 (C-4), and 83.6 (C-7)] (Table 1). HMBCs from H-2 to C-9 and from H-3 to C-8 and C-9 established a 2,3-substitued pyrrole ring, and the molecular formula suggested that the pyrrole ring is incorporated into an 4,5,6,7-tetrasubstituted indole skeleton (Figure 1A). In the remaining formula of $CH_2Br_2O_2$, deshielded chemical shifts of the methylene group (δ_H 6.07; δ_C 101.5) indicated the existence of a methylenedioxy moiety (Figure 1B). Among the non-protonated carbons, δ_C 83.6, 91.6, 141.4, and 142.7, two bromine atoms may be attached to the shielded carbons at δ_C 83.6 and 91.6 because of the heavy atom effect. An HMBC from H-3 to C-4 (δ_C 91.6) showed that a bromine is attached to C-4. The HMBCs from H_2-10 (δ_H 6.07) to the carbons at δ_C 141.4 and 142.7 suggested candidate models ***a*** and ***b*** (Figure 1B). Although ***a*** was preferable to ***b*** based on the chemical shifts, time-dependent density-functional theory (TDDFT) calculations of the ^{13}C NMR data were conducted to confirm this (Table S1).[8] As shown in Figure 1C, the calculated values for ***a*** matched the experimental data ($R^2 = 0.9969$) whereas the correlation between the calculated and experimental data for ***b*** was low ($R^2 = 0.9285$). Thus, model ***a*** was found to be the most likely isomer.

Table 1. ^{1}H and ^{13}C NMR Data of **1** ($CDCl_3$).

No.	δ_C, type	δ_H, mult.	HMBC
1		8.30, br s	
2	123.5, CH	7.15, br s	3, 9
3	103.9, CH	6.55, br s	2, 4, 8, 9
4	91.6, C		
5	142.7 [a], C		
6	141.4 [a], C		
7	83.6, C		
8	129.4, C		
9	122.9, C		
10	101.5, CH_2	6.07, s	5, 6

[a] May be interchanged.

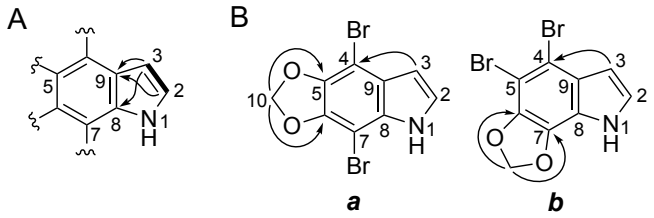

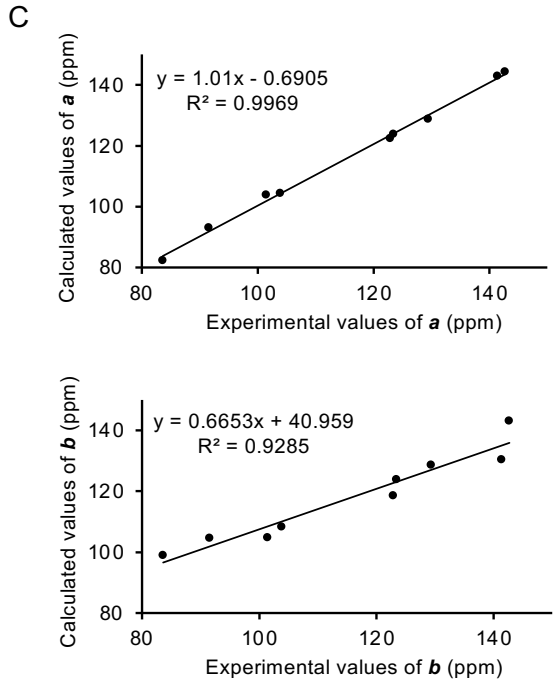

Figure 1. (A) COSY correlations (solid line) and key HMBCs (arrows) of the partial structure of **1**. (B) Candidate models ***a*** and ***b*** for **1** with HMBCs. (C) Correlations of experimental versus calculated ^{13}C NMR chemical shifts of models ***a*** and ***b***.

To confirm the structure of **1**, a total synthesis was performed. Initially, a direct dibromination reaction was attempted using commercially available 5,6-methylenedioxyindole (**2**) as a substrate (Scheme 1A). However, although the major brominated product **3** contained two bromine atoms, its ^{1}H NMR spectrum did not match that of **1**, and HMBC correlations showed that **3** was a 2,3-dibromo derivative. Therefore, the synthetic plan was switched to introduce the two bromine atoms before constructing the highly reactive pyrrole ring (Scheme 1B). Commercially available 6-nitropiperonal (**4**) was treated with 4 equiv. of *N*-bromosuccinimide (NBS) in concentrated H_2SO_4 to provide a 63% yield of dibromobenzene derivative **5**.[9] Next, the Henry reaction was carried out using Al_2O_3 as the base in the presence of nitromethane followed by a dehydration reaction using acetic anhydride to afford dinitro compound **6** in good conversion. Since compound **6** was extremely crystalline and the crystals were difficult to be dissolved in any solvent, and then the crude product containing **6** was directly employed in an indole construction reaction by reduction with an excess amount of iron in acetic acid[10] to finally obtain an excellent yield of **1** in gram scale quantities (56% over three-steps). All spectroscopic data, including the ^{1}H and ^{13}C NMR spectra, of synthetic **1** (Figures S21 and S22) were validated with the data of naturally occurring **1**.

Scheme 1. (A) Direct Dibromination of 2 and HMBCs (Arrows) for 3. (B) Total Synthesis of Amakusamine (1)

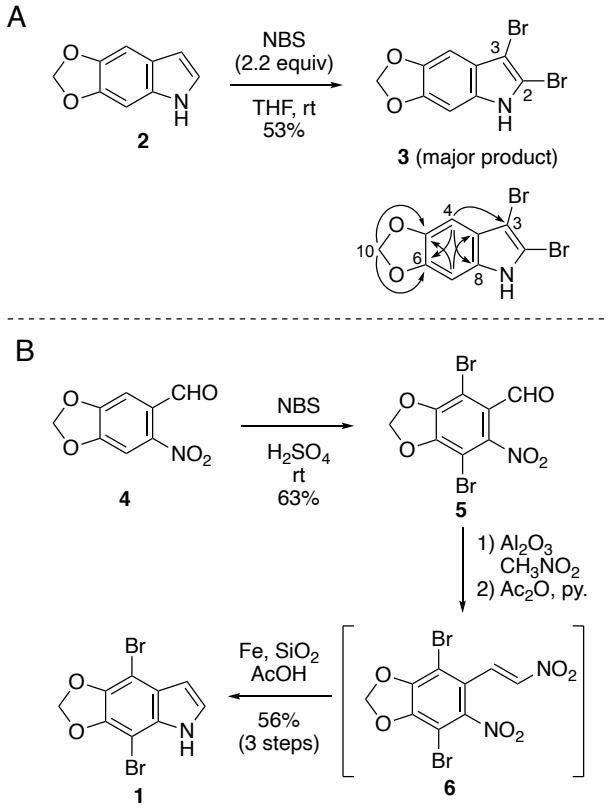

The biological activity of **1** was evaluated with our in-house screening including cytotoxicity, antimicrobial activities, inhibition of the RANKL-induced formation of multinuclear osteoclasts, and inhibition of the ubiquitin–proteasome system [proteasome, E1, Ubc13 (E2)–Uev1A interaction, p53–Mdm2 (E3) interaction, and USP7]. Among these, **1** inhibited the RANKL-induced formation of multinuclear osteoclasts in RAW264 cells. RANKL induces the differentiation of RAW264 cells to mononuclear osteoclasts, which is associated with up-regulation of several downstream signaling pathways such as the NF-κB and mitogen-activated protein kinase (MAPK) signaling pathways, followed by inducing the expression of osteoclast-specific genes encoding tartrate-resistant acid phosphatase (TRAP), a marker of osteoclastogenesis, and enzymes involved in cell fusion. After treatment with RANKL (50 ng/mL) in the presence or absence of **1**, cells were allowed to differentiate for 4 days. Cells in the

presence of RANKL that had been induced to become TRAP-positive osteoclasts were stained red with TRAP-staining solution (Figure 2A), and the number of multinuclear osteoclasts (containing three or more nuclei) were counted.[11] Natural **1** inhibited the formation of multinuclear osteoclasts in a concentration-dependent manner with an IC_{50} value of 10.5 μM (Figures 2A,B), and synthetic **1** showed equivalent efficacy (IC_{50}, 9.4 μM). Next, the effect of **1** on the expression of osteoclastogenic specific genes was evaluated. Total RNA was prepared and analyzed by real-time RT-PCR. Nuclear factor of activated T cells c1 (NFATc1) is known to be a master regulator of osteoclastogenesis and regulates the expression of various osteoclast-specific factors.[12] RANKL (50 ng/mL) induced the expression of *Nfatc1*, and synthetic **1** showed a concentration-dependent suppression of the gene (Figure 2C), indicating that **1** inhibits the activation of the NFATc1 signaling pathway.

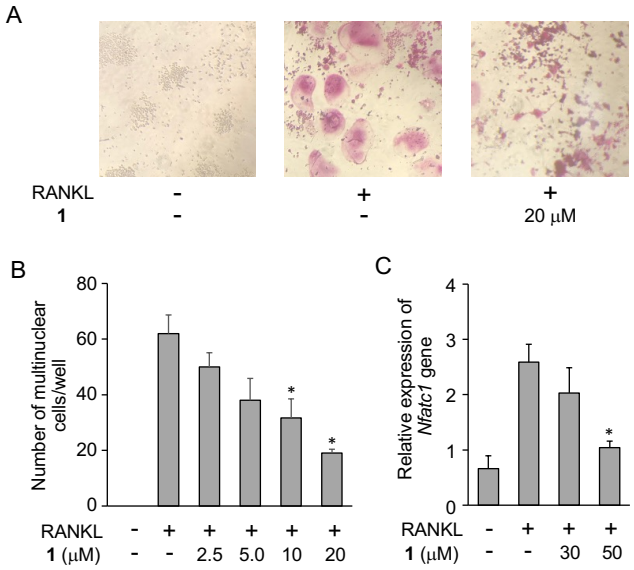

Figure 2. Effects of **1** on RANKL-induced osteoclastogenesis in RAW264 cells. (A) Cells were incubated with RANKL (50 ng/mL) in the presence or absence of natural **1** at 20 μM for 4 days. The cells were stained with TRAP-staining solution. (B) After treatment with natural **1** at the indicated concentrations, TRAP-positive multinuclear osteoclasts (nuclei ≥ 3) were stained red

and counted. (C) RAW264 cells treated with RANKL (50 ng/mL) in the presence or absence of synthetic **1** (30 or 50 μM) were incubated for 24 h. Total RNA was extracted and mRNA expression of *Nfatc1* was evaluated by real-time RT-PCR. The results are expressed as means ± SD (n=3). *$p < 0.05$ versus the control.

The structure of **1** reveals it to be a simple indole derivative, which inhibited the formation of multinuclear osteoclasts. Then, we conducted SAR studies with a commercially available **2** and 15 synthetic derivatives (**3** and **7**–**20**) (see details in Supporting Information) (Figure 3) as follows: 1) First, the effect of a Δ^2 double bond was tested with **7**. This reduced its IC_{50} value to 25.6 μM, indicating that the presence of the double bond is important for activity; 2) Next, a methylenedioxy group was replaced with two methoxy groups (**8**),[9] which slightly enhanced its activity; 3) The effect of the bromine atoms on the indole skeleton was assessed. A compound without bromines (**2**) showed no inhibition even at 50 μM. Compounds **9** and **10** with one bromine at C-4 and C-7, respectively, were less potent than **1** [IC_{50} = 16.8 (**9**) and 35.4 (**10**) μM]. Compound **3** with bromines at C-2 and C-3 showed 40% inhibition at 50 μM, and **11** with chlorines at C-4 and C-7 instead of bromines showed weaker activity (IC_{50} = 40.0 μM). These results indicate that a bromine at C-4 is essential (**9**) and the bromine at C-7 slightly enhances efficacy (**10** versus **2**). Replacement of the bromines with chlorines significantly reduced activity (**1** versus **11**), but the presence of the chlorines slightly improved efficacy compared with the absence of bromines (**11** versus **2**); 4) The potencies of *N*-acyl derivatives were evaluated. Those with C_2–C_8-alkyl chains (**12**–**14**) were equipotent or slightly more potent (IC_{50} = 7.9–11.7 μM), but that with C_{14}-alkyl chain (**15**) and benzoyl derivative **16** had no activity; 5) For substituents at C-3, methyl (**17**) and hydroxymethyl (**18**) derivatives were slightly more potent or equipotent

[IC_{50} = 8.1 (**17**) and 10.0 (**18**) μM], but formyl derivative **19** was less potent (IC_{50} = 13.9 μM). Aminoethyl derivative **20**, a tryptamine derivative, was more potent but showed cytotoxicity at 25 μM. None of the other derivatives showed toxicity even at 50 μM. These results indicate that substituents on the indole core of **1** affect its inhibition of RANKL-induced osteoclastogenesis in RAW264 cells, and that the presence of bromine atoms is necessary for this activity. Further investigations are needed for the development of more potent derivatives based on **1** for the prevention and treatment of osteoporosis.

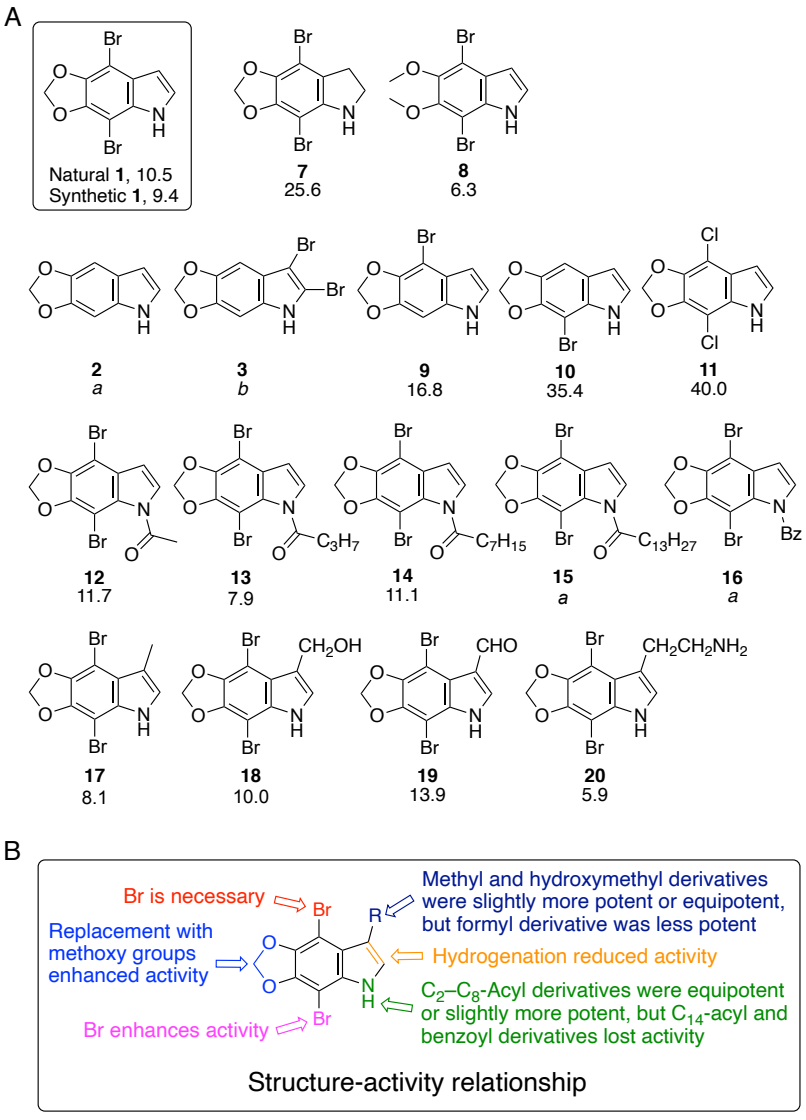

Figure 3. (A) Inhibition (IC_{50}, μM) of RANKL-induced osteoclastogenesis in RAW264 cells of natural and synthetic **1** and 16 derivatives. [a] Compounds showed no inhibition even at 50 μM. [b] Compound showed 40% inhibition at 50 μM. (B) Summary of the SAR of **1** and its derivatives as RANKL-induced osteoclastogenesis inhibitors.

Indole is known to be produced from L-tryptophan in Gram-positive and Gram-negative bacteria,[13,14] regulating diverse bacterial processes, such as biofilm formation, virulence, cell adherence, and drug resistance in indole-producing bacteria.[15] Recent studies have shown that indole also affects the physiology and behavior of non-indole-producing species and eukaryotes. Furthermore, these organisms metabolize indole into various derivatives via their own metabolic pathways, and such derivatives have diverse functions in these organisms.[15] Amakusamine (**1**) may also be formed from L-tryptophan by degradation followed by bromination and oxidation/methylation.

Amakusamine (**1**) is a simple methylenedioxy dibromoindole alkaloid isolated from a sponge. Marine-derived indole alkaloids form a large family of bioactive secondary metabolites.[16] Among these, 3,6-dibromoindole[17] and polybrominated bis-indoles[18] from an ascidian and a marine cyanobacterium, respectively, are known to be simple bromoindole alkaloids. From plants, clausenalene[19] and orisuaveoline B[20] are methylenedioxy indole alkaloids without bromines. Amakusamine (**1**) is the first methylenedioxy bromoindole alkaloid with anti-osteoporosis activity, which may serve as a new scaffold for drug development.

EXPERIMENTAL SECTION

General Experimental Procedures. UV spectra were measured on a JASCO V-550 spectrophotometer in MeOH. IR spectra were recorded on a Perkin Elmer Frontier FT-IR spectrophotometer. NMR spectra were recorded on a Bruker Avance III 600 NMR spectrometer in $CDCl_3$. Chemical shifts were referenced to the residual solvent peaks (δ_H 7.24 and δ_C 77.0 for $CDCl_3$). HRESIMS spectra was measured on a Waters Xevo G2-XS Qtof mass spectrometer. The preparative HPLC system comprised a Waters 515 HPLC pump, Waters 2489 UV/visible detector. Microscopic images were taken by Keyence BIOREVO BZ-9000.

Animal Material. The marine sponge was collected by scuba diving at a depth of 5 m in Amakusa, Kumamoto Prefecture, Japan, in September 13, 2013. The sponge was soaked in EtOH immediately after sampling and kept frozen at -20 °C until extraction. The sponge was identified as *Psammocinia* sp. by one of the authors (Y.I.). External morphology of the sponge was not recorded but the color is dark brown in ethanol. The ectosomal skeleton of the sponge couldn't be precisely observed because the surface of the sample used for identification was broken. The choanosomal skeleton contained large amount of sand grains and consist of fibers and fine filaments. Fibers are cored with sand grains and foreign spicules. Fibers didn't make peculiar mesh-like network but dichotomously divided to make skeletal structure. The fine filaments are uncored, curved, and diverged from main fibers. Fibers are 32–100 μm in diameter, and fine filaments are 6–10 μm in diameter. Until now, 37 species have been recorded as valid for the genus *Psammocinia* Lendenfeld, 1889 according to World Porifera Database.[21] Of these, *Psammocinia scopulus* Sim, Lee and Kim, 2017 once collected from Korean waters can be comparable with our specimen (13K013) for its internal skeletal characters and geographical distribution. However, *P. scopulus* has distinct fascicles made of primary fibers that is indistinct in our specimen, and the filaments are thinner (3–7μm).[22] A voucher specimen (13K013) has

been deposited in Department of Natural Medicines, Graduate School of Pharmaceutical Sciences, Kumamoto University, Japan.

Extraction and Isolation. The sponge (3.0 kg, wet weight) was extracted with EtOH and MeOH. After evaporation, the residual solution was extracted with EtOAc. The EtOAc fraction (8.7 g) was partitioned between *n*-hexane and 90% MeOH–H_2O. The aqueous MeOH fraction (6.7 g) was subjected to SiO_2 column chromatography with 75% *n*-hexane–EtOAc and CH_2Cl_2. Fraction eluted with *n*-hexane/EtOAc was purified by gel filtration HPLC (Asahipack GS-310P column, Asahi Chemical Industry Co., Ltd., 21.5 × 500 mm) with EtOAc to yield **1** (4.6 mg).

*Amakusamine (**1**):* A white solid; UV (MeOH) λ_{max} (log ε) 212 (4.5), 278 (3.9), 308 (3.9) nm; IR (film) ν_{max} 3418, 2923, 1455, 1304, 1203, 1055, 945, 833, 748, 710 cm^{-1}; ^1H and ^{13}C NMR data, Table 1; HRESITOFMS *m/z* 315.8610 $[M - H]^-$ (calcd for $C_9H_4{}^{79}Br_2NO_2$, 315.8614).

Conformational Analysis and Chemical Shift Calculations. These experiments were performed as previously described[23] using Spartan'18 instead of Spartan'16. Chemical shift calculations were performed at the wB97X-D/6-31G* level.

Formation of RANKL-induced Multinuclear Osteoclasts in RAW264 Cells. This experiment was performed as previously described.[24] Purities of natural and synthetic compounds were judged by their ^1H and ^{13}C NMR spectra.

Real-time RT-PCR analysis. RAW 264 cells seeded on a 6-well plate (2.7×10^4 cells/well) were treated with sRANKL (50 ng/mL) and **1** (30 or 50 μM) and incubated for 24 h. RNA extraction and real-time RT-PCR analysis were conducted as previously described.[25]

Cytotoxicity assay. The cytotoxicity assay was performed with RAW 264 cells using MTT.[26]

Synthesis of Amakusamine (1). To a solution of 6-nitropiperonal (**4**, 1.5 g, 7.7 mmol) in concentrated H_2SO_4 (12 mL), *N*-bromosuccinimide (5.49 g, 30.8 mmol) was slowly added at rt under Ar atmosphere. The reaction mixture was stirred for 16 h at rt. The resulting mixture was poured onto crushed ice, and the resulting solid was collected by vacuum filtration, washed with H_2O, MeOH, and *n*-hexane. Desired 4,7-dibromo-6-nitropiperonal (**5**, 1.7 g, 63%) was obtained as a pale yellow solid. All spectroscopic data of **5** were identical with reported data.[27]

To a solution of 4,7-dibromo-6-nitropiperonal (**5**, 1.95 g, 5.5 mmol) in nitromethane (24 mL), Al_2O_3 (1.7 g, 16.7 mmol) was added at rt under Ar atmosphere. The reaction mixture was stirred for 12 h at rt. The resulting mixture was filtrated with Celite pad and following a silica gel pad with $CHCl_3$. The resulting solution was concentrated under reduced pressure. The residue was dissolved in acetic anhydride (22 mL) and pyridine (2.3 mL, 28 mmol) was added to the resulting mixture at rt under Ar atmosphere. The reaction mixture was stirred for 12 h at rt. The resulting mixture was quenched with saturated aqueous $NaHCO_3$ solution. The aqueous layer was extracted three times with $CHCl_3$. The combined organic layer was dried over $MgSO_4$, and concentrated under reduced pressure. The crude materials of **6** was dissolved to benzene (35 mL) and cyclohexane (15 mL), then, acetic acid (33 mL), silica gel (5.5 g) and iron (4.3 g, 78 mmol) were added to the mixture at rt under Ar atmosphere. The reaction mixture was warmed up to 100 °C, and stirred for 40 min at 100 °C. After cooling to rt, the resulting mixture was filtrated with Celite pad with $CHCl_3$. The organic layer was washed with saturated brine, saturated $NaHSO_3$ solution, and saturated $NaHCO_3$ solution. The combined organic layer was dried over $MgSO_4$, and concentrated under reduced pressure. The crude materials were purified by flash chromatography (SiO_2, 25% $CHCl_3$/*n*-hexane) to provide amakusamine (**1**) (991 mg, 53%, 3

steps) as white crystals. All spectroscopic data were identified with the data of naturally occuring **1**.

*Synthetic **1**:* White crystals; mp 215–220 °C; IR (neat) ν_{max} 3420, 1454, 1303, 1202, 1078, 1055, 941, 831, 748, 710 cm^{-1}; ^1H NMR (600 MHz, $CDCl_3$) δ 8.30 (br. s, 1H), 7.17 (t, J = 3.0 Hz, 1H), 6.57 (t, J = 3.0 Hz, 1H), 6.09 (s, 2H); ^{13}C NMR (150 MHz, $CDCl_3$) δ 142.9, 141.5, 129.6, 123.7, 123.0, 104.1, 101.7, 91.7, 83.7; HRESIMS *m/z* 317.8775 $[M + H]^+$ (calcd for $C_9H_6{}^{79}Br_2NO_2$, 317.8760).

ASSOCIATED CONTENT

Supporting Information

The Supporting Information is available free of charge at https://pubs.acs.org/doi/10.1021/acs.jnatprod.xxxxxxx.

Experimental procedures; NMR spectra of **1** and synthetic compounds; calculated ^{13}C NMR data of models ***a*** and ***b*** (PDF)

Notes

The authors declare no competing financial interest.

ACKNOWLEDGMENT

This work was supported by JSPS KAKENHI Grants JP20H03396 (S.T.), JP18K06719 (H.K.), JP20K16026 (Y.H.), and JP21H02608 (H.I.) and Useful and Unique Natural Products for Drug Discovery and Development (UpRod), Program for Building Regional Innovation Ecosystems at Kumamoto University, Japan.

REFERENCES

(1) Carroll, A. R.; Copp, B. R.; Davis, R. A.; Keyzers, R. A.; Prinsep, M. R. Marine natural products. *Nat. Prod. Rep.* **2021**, *38*, 362–413.

(2) Munro, M. H. G.; Blunt, J. W.; Dumdei, E. J.; Hickford, S. J. H.; Lill, R. E.; Li, S.; Battershill, C. N.; Duckworth, A. R. The discovery and development of marine compounds with pharmaceutical potential. *J. Biotechnol*. **1999**, *70*, 15–25.

(3) Gribble, G. W. The natural production of organobromine compounds. *Environ. Sci. Pollut. Res.* **2000**, *7*, 37–49.

(4) Boyle, W. J.; Simonet, W. S.; Lacey, D. L. Osteoclast differentiation and activation. *Nature* **2003**, *423*, 337−342.

(5) Takayanagi, H. Osteoimmunology: shared mechanisms and crosstalk between the immune and bone systems. *Nat. Rev. Immunol.* **2007**, *7*, 292−304.

(6) Boyce, B. F. Advances in the regulation of osteoclasts and osteoclast functions. *J. Dent. Res.* **2013**, *92*, 860−867.

(7) Rachner, T. D.; Khosla, S.; Hofbauer, L. C. Osteoporosis: now and the future. *Lancet* **2011**, *377*, 1276−1287.

(8) Lodewyk, M. W.; Siebert, M. R.; Tantillo, D. J. Computational prediction of ^{1}H and ^{13}C chemical shifts: a useful tool for natural product, mechanistic, and synthetic organic chemistry. *Chem. Rev.* **2012**, *112*, 1839–1862.

(9) Huleatt, P. B.; Lau, J.; Chua, S.; Tan, Y. L.; Doung, H. A.; Chai, C. L. L. Concise, efficient and practical assembly of bromo-5,6-dimethoxyindole building blocks. *Tetrahedron Lett.* **2011**, *52*, 1339–1342.

(10) Fukuyama, Y.; Iwatsuki, C.; Kodama, M.; Ochi, M.; Kataoka, K.; Shibata, K. Antimicrobial indolequinones from the mid-intestinal gland of the muricid gastropod *Drupella fragum*. *Tetrahedron* **1998**, *54*, 10007–10016.

(11) Tsukamoto, S.; Takeuchi, T.; Kawabata, T.; Kato, H.; Yamakuma, M.; Matsuo, K.; El-Desoky, A. H.; Losung, F.; Mangindaan, R. E. P.; de Voogd, N. J.; Arata, Y.; Yokosawa, H. Halenaquinone inhibits RANKL-induced osteoclastogenesis. *Bioorg. Med. Chem. Lett.* **2014**, *24*, 5315–5317.

(12) Asagiri, M.; Takayanagi, H. The molecular understanding of osteoclast differentiation. *Bone* **2007**, *40*, 251–264.

(13) Smith, T. A modification of the method for determining the production of indol by bacteria. *J. Exp. Med.* **1897**, *2*, 543–547.

(14) Deeley, M. C.; Yanofsky, C. Nucleotide sequence of the structural gene for tryptophanase of *Escherichia coli* K-12. *J. Bacteriol.* **1981**, *147*, 787–796.

(15) Lee, J. H.; Lee, J. Indole as an intercellular signal in microbial communities. *FEMS Microbiol. Rev.* **2010**, *34*, 426–444.

(16) Netz, N.; Opatz, T. Marine indole alkaloids. *Mar. Drugs* **2015**, *13*, 4814–4914.

(17) Qureshi, A.; Faulkner, D. J. 3,6-Dibromoindole, a new indole from the Palauan ascidian *Distaplia regina*. *Nat. Prod. Lett.* **1999**, *13*, 59–62.

(18) Norton, R. S.; Wells, R. J. A Series of chiral polybrominated biindoles from the marine blue-green alga *Rivularia firma*. Application of ^{13}C NMR spin-lattice relaxation data and coupling constants to structure elucidation. *J. Am. Chem. Soc.* **1982**, *104*, 3628–3635.

(19) Bhattacharyya, P.; Biswas, G. K.; Barua, A. K.; Saha, C.; Roy, I. B.; Chowdhury, B. K. Clausenalene, a carbazole alkaloid from *Clausena heptaphylla*. *Phytochemistry* **1993**, *33*, 248–250.

(20) Wansi, J. D.; Mesaik, M. A.; Chiozem, D. D.; Devkota, K. P.; Gaboriaud-Kolar, N.; Lallemand, M. C.; Wandji, J.; Choudhary, M. I.; Sewald, N. Oxidative burst inhibitory and cytotoxic indoloquinazoline and furoquinoline alkaloids from *Oricia suaveolens*. *J. Nat. Prod.* **2008**, *71*, 1942–1945.

(21) de Voogd, N. J.; Alvarez, B.; Boury-Esnault, N.; Carballo, J. L.; Cárdenas, P.; Díaz, M. -C.; Dohrmann, M.; Downey, R.; Hajdu, E.; Hooper, J. N. A.; Kelly, M.; Klautau, M.; Manconi, R.; Morrow, C. C.; Pisera, A. B.; Ríos, P.; Rützler, K.; Schönberg, C.; Vacelet, J.; van Soest, R. W. M. (2021). World Porifera Database. *Psammocinia* Lendenfeld, 1889. http://www.marinespecies.org/porifera/porifera.php?p=taxdetails&id=165060 on 2021-09-17 (Accessed 15 September 2021).

(22) Sim, C. J.; Lee, K. J.; Kim, Y. A. New species in two genera, *Psammocinia* and *Ircinia* (Demospongiae: Dictyoceratida: Irciniidae), from Korea. *Journal of Species Research* **2017**, *6* (Special Edition), 94–109.

(23) Torii, M.; Kato, H.; Hitora, Y.; Angkouw, E. D.; Mangindaan, R. E. P.; Voogd, N. J. D.; Tsukamoto, S. Lamellodysidines A and B, sesquiterpenes isolated from the marine sponge *Lamellodysidea herbacea*. *J. Nat. Prod.* **2017**, *80*, 2536−2541.

(24) Tsukamoto, S.; Takeuchi, T.; Kawabata, T.; Kato, H.; Yamakuma, M.; Matsuo, K.; El-Desoky, A. H.; Losung, F.; Mangindaan, R. E. P.; de Voogd, N. J.; Arata, Y.; Yokosawa, H. Halenaquinone inhibits RANKL-induced osteoclastogenesis. *Bioorg. Med. Chem. Lett.* **2014**, *24*, 5315–5317.

(25) Kato, H.; Kai, A.; Kawabata, T.; Sunderhaus, J. D.; Mcafoos, T. J.; Finefield, J. M.; Sugimoto, Y.; Williams, R. M.; Tsukamoto, S. Enantioselective inhibitory abilities of enantiomers of notoamides against RANKL-induced formation of multinuclear osteoclasts. *Bioorg. Med. Chem. Lett.* **2017**, *27*, 4975−4978.

(26) Afifi, A. H.; El-Desoky, A. H.; Kato, H.; Mangindaan, R. E. P.; de Voogd, N. J.; Ammar, N. M.; Hifnawy, M. S.; Tsukamoto, S. Carteritins A and B, cyclic heptapeptides from the marine sponge *Stylissa carteri*. *Tetrahedron Lett.* **2016**, *57*, 1285–1288.

(27) Raju, P.; Rajeshwaran, G. G.; Nandakumar, M.; Mohanakrishnan, A. K. Unusual reactivity of aryl aldehydes with triethyl phosphite and zinc bromide: A facile preparation of epoxides, benzisoxazoles, and α-hydroxy phosphonate ester. *Eur. J. Org. Chem.* **2015**, 3513–3523.

Table of Contents/Abstract Graphic

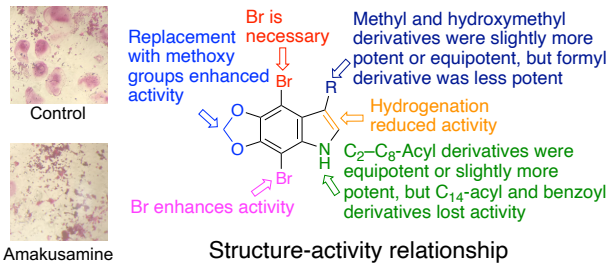

Structure-activity relationship